$Ni(C_2H_4)_2$ the ethylenes were held only very weakly in the coordination sphere with optimized Ni–C distances greater than 2.30 Å in all cases. The Ni–C distances for the three-coordinate complexes were 2.04 Å (**14a**) and 2.12 Å (**14b**).

The optimized angular disposition of the phosphines are given in the diagrams throughout the text.

The reaction coordinate for the elimination of cyclobutane was studied using the metallacycle framework **21**. The Ni–X distance

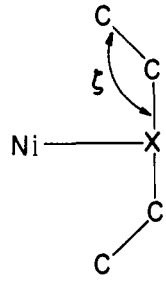

21

was increased stepwise and the angle ζ and the positions of the other ligands were optimized. The reaction coordinate for the fragmentation of the metallacycle to ethylene was studied using **22**, similar to that used by Stockis and Hoffmann.[4] The angle

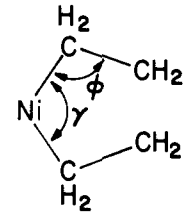

22

γ was opened stepwise and ϕ and ligand position were optimized.

Acknowledgments. We thank Professors R. H. Grubbs and H. B. Gray for helpful comments. The Cornell group thanks the National Science Foundation for support through Research Grant CHE 7828048.

Thermochromic Phase Transitions in Copper(II) Halide Salts. 1. Crystal Structure and Magnetic Resonance Studies of $(CH_3)_2CHNH_3CuCl_3$

S. A. Roberts, D. R. Bloomquist, R. D. Willett,* and H. W. Dodgen

Contribution from the Department of Chemistry, Washington State University, Pullman, Washington 99164. *Received June 16, 1980*

Abstract: $(CH_3)_2CHNH_3CuCl_3$ undergoes a thermochromic phase change at T_{th} = 51 °C changing in color from brown to orange. The low-temperature phase (II) is triclinic of space group $P\bar{1}$ with a = 11.692 (8) Å, b = 7.804(4) Å, c = 6.106 (3) Å, α = 79.00 (4)°, β = 122.60 (4)°, and γ = 116.47 (4)° with Z = 2. The high-temperature phase (I) is orthorhombic *Pcan* with a = 17.589 (7) Å, b = 7.296 (3) Å, and c = 6.365 (3) Å with Z = 4. Phase II contains bibridged linear chains of $Cu_2Cl_6^{2-}$ dimers; phase I contains tribridged chains of $(CuCl_3)_n^{n-}$ stoichiometry. The chain axes are coincident in the two phases. The $(CH_3)_2CHNH_3^+$ (IPA) ions are ordered in phase II but disordered in phase I. The ^1H NMR line width narrows at T_{th} to 4.5 G for the N-deuterated salt, consistent with a dynamic twofold disorder of the IPA ion. Single-crystal EPR data at 78 K are consistent with the structure of phase II. Susceptibility studies show the phase II linear chain consists of antiferromagnetically coupled dimers with an S = 0 ground state while the phase I linear chain is ferromagnetically coupled. A sharp break in the susceptibility occurs at T_{th}, indicating the existence of a first-order phase transition. Deuteration of the NH_3^+ moiety *raises* T_{th} by 10 °C, indicating the presence of weaker N–H···Cl hydrogen bonds in phase I. This weaker hydrogen bond allows the copper(II) ions to *increase* their coordination and form the more compact tribridged chain. Concommitantly, the barrier to rotation is lowered, and the cation becomes disordered.

The most easily detected solid-state phase transitions are those in which the color of the crystals change as the temperature is either raised or lowered. This thermochromism can be of two types. Continuous thermochromism is characterized by a gradual change in crystal color and is not indicative of a phase transition. On the other hand, discontinuous thermochromic phase transitions are evidenced by a dramatic change in crystal color at some temperature (T_{th}) and are symptomatic of a sudden change in crystal properties at T_{th}. In transition-metal complexes, thermochromism is a sign of a change in ligand coordination. These transformations may include alterations in atom connectivity, or they may only represent geometric distortions in the preexisting chemical entities.

Mori and co-workers[1] report studies on halogen-substituted dinitrodiamminecopper(II) compounds showing this thermochromism to be a result of coordinate isomerization of the ambidentate NO_2 ligand. At low temperatures, the pure dinitrodiamminecopper(II) is purple and contains N-bonded NO_2 groups, while at high temperatures the green complexes contain O-bonded NO_2 ligands. As halides are doped into the salt, T_{th} is lowered until some critical halide concentration is reached and the green complexes are stabilized at all temperatures.

Various bis(*N*-alkylethylenediamine)copper(II) salts are also thermochromic.[2-5] The red, low-temperature phase contains

(1) Y. Mori, H. Inoue, and M. Mori, *Inorg. Chem.*, **14**, 1002 (1975).

(2) A. B. P. Lever, E. Mantovani, and J. C. Donini, *Inorg. Chem.*, **10**, 2424 (1971).

(3) L. Fabbrizzi, M. Micheloni, and P. Paoletti, *Inorg. Chem.*, **13**, 3019 (1974).

(4) J. R. Farraro, L. J. Basile, L. R. Garcia-Ineguez, P. Paoletti, and L. Fabbrizzi, *Inorg. Chem.*, **15**, 2342 (1976).

(5) J. R. Ferraro, L. Fabbrizzi, and P. Paoletti, *Inorg. Chem.*, **16**, 2127 (1977).

0002-7863/81/1503-2603$01.25/0

nearly square-planar $Cu(en)^{2+}$ ions and uncoordinated anions. The ethylenediamine rings are in their most stable configuration, and in this form, the alkyl groups on the nitrogen atom block the anion's approach to the fifth and sixth coordination positions. In the violet, high-temperature form, the alkyl groups are disordered, weakening the ligand field strength of the amine ligands.

In copper halide salts, discontinuous thermochromism has been known for some time.[6] For $CuCl_4^{2-}$ salts, if the cation is bulky enough to prevent stabilization of the normal two-dimensional layer structure, phase transitions will frequently occur upon changes in either pressure or temperature. It is well characterized in $CuCl_4^{2-}$ salts that the green to yellor color change is the result of relaxation of anion geometry from a sterically crowded square-planar arrangment of ligands to a less constrained distorted tetrahedral configuration.[7-11] Indeed, the color is such a sensitive indicator of anion geometry that schemes have been put forth to determine the structure of the anion from its electronic spectrum alone.[7-9]

When $CuCl_4^{2-}$ geometry is described, a parameter used to characterize the complex structure is θ, the average of the trans angles in the complex. If the angle between each pair of ligand Cl atoms is computed, two of the angles are generally similar in size and larger than 110°, with $\theta = 180°$ for square-planar complexes, less than this if the complex is distorted toward tetrahedral geometry, and 109.5° for a tetrahedral ion. The average of these two large angles is θ.

Among the cations for which thermochromic tetrachlorocuprate(II) salts have been found are the isopropylammonium,[7] diethylammonium,[7] *N*-methylphenethylammonium,[12] and piperazinium.[13] In each case, spectroscopic evidence shows that the low-temperature form contains relatively planar $CuCl_4^{2-}$ ions which at T_{th} relax to a more tetrahedral $CuCl_4^{2-}$ configuration with approximate D_{2d} symmetry. These results are in agreement with calculations on the isolated $CuCl_4^{2-}$ ion which indicate an intrinsic distortion from tetrahedral geometry, having a stable configuration with θ near 130°.[14] In the high-temperature forms of these thermochromic salts, hydrogen-bonding and crystal-packing forces are weakened to the point where this intrinsic stability outweighs other considerations and the phase transition occurs.

A_2NiCl_4 complexes eluded synthesis for many years, but after first developing a melt technique, Ferraro[15] has prepared an exhaustive series of tetrachloronickelate(II) salts, all of which are thermochromic. The geometry change at the phase transition, as characterized by spectroscopic methods, is from a polymeric chloro-bridged relatively planar $NiCl_4^{2-}$ species to discrete, tetrahedral $NiCl_4^{2-}$ ions above T_{th}. The effect of greater cation hydrogen-bonding ability is to raise T_{th}. Thermochromism in this type of salt must be more complicated than in the salts containing isolated $CuCl_4^{2-}$ ions as the ligand bridges must dissociate.

In this paper, the results of the study of the thermochromic salt isopropylammonium trichlorocuprate(II), ($IPACuCl_3$), is reported. This salt has been subjected to less previous study than any of the other compounds described in this work. It was first prepared by Remy and Laves,[6] who noted the thermochromism. A later systematic study of the electronic absorption spectra of copper chloride dimers included the $IPACuCl_3$ salt and showed that its spectrum is characteristic of a planar $Cu_2Cl_6^{2-}$ dimer;[16] that is a flat-bibridged dimer having a square-planar arrangement of chloride ligands about the central copper ions which each have zero, one, or two long axial contacts with chloride ions in adjacent dimers. Magnetic susceptibility measurements through the phase transition, to be discussed in more detail later, show a discontinuity at T_{th}.[17] X-ray crystallographic, magnetic resonance, and magnetic susceptibility methods were used in an attempt to characterize the nature of each phase and to elucidate the mechanism or reason for the transition. Also, as copper halide salts are useful approximations of magnetic model systems, the low-temperature magnetic susceptibility and EPR behavior of both phases of $IPACuCl_3$ have been studied.

Experimental Section

Crystal Preparation. $IPACuCl_3$ was prepared by the method of Remy and Laves[6] by dissolution of equimolar amounts of isopropylammonium chloride and $CuCl_2 \cdot 2H_2O$ in ethanol followed by slow evaporation until crystallization occurred.

The deuterated salt was prepared by dissolving the starting materials in sufficient D_2O to exchange 98% of the ammonium protons and evaporating the solution in a dessicator to dryness. This compound, D-$IPACuCl_3$, is also thermochromic, but T_{th} has increased 10 °C.

DTA and DSC measurements were made on a Du Pont 900 thermal analyzer. Values obtained for T_{th} were consistently 20–30 °C higher than those obtained by other methods due to superheating effects. Thermodynamic values obtained are $\Delta H_{th} = 1.4$ (2) kcal/mol, $\Delta S_{th} = 4.3$ (6) eu, $\Delta H_{mp} = 6.5$ (2) kcal/mol, and $\Delta S_{mp} = 14.4$ (6) eu. Results for the deuterated sample were identical with those for the nondeuterated sample, except that the transition occurs about 10 °C higher in temperature.

Structure Determination of Phase II. The $IPACuCl_3$ crystals grown from solution in the room-temperature phase (II) are prismatic and elongated in the *c* direction. A crystal of dimensions 0.28 × 0.09 × 0.12 mm was mounted on a glass fiber to rotate about its needle axis. Weissenberg photographs showed the crystal to be triclinic. Cell parameters calculated from least-squares refinement of 12 centered reflections were $a = 11.692$ (8) Å, $b = 7.804$ (4) Å, $c = 6.106$ (3) Å, $\alpha = 79.00$ (4)°, $\beta = 122.60$ (4)°, and $\gamma = 116.47$ (4)°. For $Z = 2$, one dimer per unit cell, the calculated density is 1.82 g/cm^3.

Intensity data were collected on an automated Picker four-circle diffractometer using Zr-filtered MoKα radiation. A total of 1446 unique reflections were collected in the range $5° \le 2\theta \le 50°$ by using a θ–2θ scan with scan width of 1.7°, 20 steps/deg, and 3 s/step counting time. The standard deviation of each reflection was calculated as $\sigma^2(I) = TC + BG + (\rho I)^2$, where TC is total counts, BG is background counts, and I is the net intensity (TC – BG), and ρ, a parameter to correct for instrumental uncertainties, was set to 0.03. The intensities of three standard reflections were monitored every 75 reflections.

Statistical analysis of the data indicated the centric space group $P\bar{1}$. Data were corrected for absorption ($\mu = 35.5$ cm^{-1}, transmission factors ranged from 0.65 to 0.74). Positions of the copper and chlorine atoms were deduced from a Patterson map, and the remaining atom positions were determined from subsequent difference syntheses. Refinement of all parameters except hydrogen thermal parameters (with B's fixed at 6.0) resulted in final residuals for all reflections of $R = 0.043$ and $wR = 0.051$, where R is defined as $\sum(|F_o - F_c|)/\sum|F_o|$, wR is defined as $[\sum w(F_o - F_c)^2/(\sum wF_o^2)]^{1/2}$, and $w = 1/\sigma^2(F)$. Maximum parameter shifts on the last cycle were half of their estimated standard deviations. Computer programs used are part of a local library.[18] Final positional and thermal parameters are listed in Table I. A table of observed and calculated structure factors is available.

Structure Determination of Phase I. The crystal used for low-temperature data collection was mounted on the diffractometer, and the instrument angles set so that a strong axial reflection of the low-temperature phase was being monitored. A dried, heated air stream was directed at the crystal. As mentioned above, the crystal was only mounted upon a glass fiber, not in a capillary, but other than drying the air stream with $CaCl_2$, no precautions against deliquescence were taken. As the crystal was warmed, the intensity of this reflection decreased by 25% until the phase transformation occurred, identified by the color change in the crystal, at which time the intensity at the set instrument angles dropped to background. The crystal was held above T_{th} from this time until the end of the data collection. Temperature was monitored during the experiment at the mouth of the hot-air tube by a chromel-alumel thermocouple and remained at 80 ± 2 °C. After completion of data collection, the thermocouple junction was moved to the position the crystal had been occupying. The temperature was 60 °C.

(6) H. Remy and G. Laves, *Ber. Dtsch. Chem. A*, **66**, 401 (1933).
(7) R. D. Willett, J. A. Haugen, J. Lebsack, and J. Morrey, *Inorg. Chem.*, **13**, 2510 (1974).
(8) J. Lamotte-Brasseur, *Acta Crystallogr. Sect. A*, **A30**, 487 (1974).
(9) R. L. Harlow, W. J. Wells, III, G. W. Watt, and S. H. Simonsen, *Inorg. Chem.* **14**, 1768 (1975).
(10) D. N. Anderson and R. D. Willett, *Inorg. Chem. Acta*, **8**, 167 (1974).
(11) R. L. Harlow and S. H. Simonsen, Winter 1977, American Crystallographic Association Meeting, Abstract No. HN5.
(12) R. L. Harlow, W. J. Wells, III, G. W. Watt, and S. H. Simonsen, *Inorg. Chem.*, **13**, 2106 (1974).
(13) G. Marcotrigiano, L. Menaube, and G. C. Pellacani, *Inorg. Chem.*, **15**, 2333 (1976).
(14) D. W. Smith, *Coord. Chem. Rev.*, **21**, 93 (1976).
(15) J. R. Ferraro and A. T. Sherren, *Inorg. Chem.*, **17**, 2499 (1978).
(16) O. L. Liles and R. D. Willett, *Inorg. Chem.*, **6**, 1666 (1967).
(17) M. Ahmed, M.S. Thesis, University of Cairo, 1975.
(18) S. A. Roberts and J. J. Willett, Washington State University Crystallographic Program Documentation, Unpublished, 1977.

Table I. Final Positional and Thermal Parameters for $IPACuCl_3$ Phase II

atom	x	y	z	$B(1,1)$	$B(2,2)$	$B(3,3)$	$B(1,2)$	$B(1,3)$	$B(2,3)$
Cu	0.5659 (1)	0.6086 (1)	0.7874 (1)	0.0099 (1)	0.0096 (1)	0.0216 (3)	0.0044 (1)	0.0082 (1)	0.0054 (1)
Cl(1)	0.4446 (2)	0.6568 (2)	0.3472 (3)	0.0166 (2)	0.0133 (3)	0.0257 (6)	0.0095 (2)	0.0116 (3)	0.0073 (3)
Cl(2)	0.6385 (2)	0.9197 (2)	0.8884 (3)	0.0119 (2)	0.0094 (3)	0.0285 (6)	0.0037 (2)	0.0107 (3)	0.0034 (3)
Cl(3)	0.6910 (1)	0.5454 (2)	0.2107 (2)	0.0097 (2)	0.0130 (3)	0.0237 (5)	0.0044 (2)	0.0075 (3)	0.0056 (3)
N	0.7025 (5)	0.1203 (7)	0.3984 (10)	0.0097 (7)	0.0160 (11)	0.0284 (22)	0.0053 (7)	0.0056 (10)	0.0034 (12)
C(1)	0.1311 (6)	0.8148 (9)	0.4508 (12)	0.0077 (7)	0.0184 (14)	0.0303 (25)	0.0024 (8)	0.0079 (12)	0.0022 (15)
C(2)	0.0987 (8)	−0.0063 (11)	0.3591 (15)	0.0140 (10)	0.0272 (18)	0.0424 (33)	0.0114 (12)	0.0119 (15)	0.0063 (19)
C(3)	0.0609 (8)	0.6727 (10)	0.2343 (15)	0.0124 (10)	0.0213 (16)	0.0398 (32)	0.0031 (10)	0.0084 (15)	−0.0042 (18)

atom[a]	x	y	z	atom[a]	x	y	z
H(1)	0.6786 (95)	0.2135 (133)	0.3458 (175)	H(6)	0.1193 (97)	0.0324 (129)	0.2418 (172)
H(2)[a]	0.6648 (92)	0.0443 (122)	0.2771 (170)	H(7)	−0.0132 (98)	0.9634 (119)	0.2701 (162)
H(3)	0.6593 (95)	0.0919 (129)	0.5209 (170)	H(8)	0.0977 (90)	0.7040 (123)	0.1029 (168)
H(4)	0.0988 (94)	0.7536 (126)	0.5909 (167)	H(9)	0.0757 (93)	0.5672 (135)	0.2762 (173)
H(5)	0.1337 (87)	0.0963 (118)	0.4988 (161)	H(10)	0.9437 (97)	0.6150 (118)	0.1104 (163)

[a] $B = 6.0000$ Å^2.

Table II. Final Positional and Thermal Parameters for $IPACuCl_3$ Phase I.

atom	x	y	z	$B(1,1)$	$B(2,2)$	$B(3,3)$	$B(1,2)$	$B(1,3)$	$B(2,3)$
Cu	0.5000	0.5000	0.0	0.0028 (1)	0.0144 (4)	0.0155 (5)	0.0009 (2)	0.0006 (1)	0.0017 (4)
Cl(1)	0.5973 (2)	0.5000	0.7500	0.0022 (1)	0.0185 (8)	0.0199 (10)	0.0	0.0	0.0024 (8)
Cl(2)	0.5569 (1)	0.7360 (4)	0.3225 (3)	0.0036 (1)	0.0170 (6)	0.0198 (7)	−0.0025 (2)	−0.0006 (2)	0.0031 (6)
N	0.4045 (6)	0.0	0.2500	0.0021 (5)	0.0280 (34)	0.0479 (46)	0.0	0.0	−0.0119 (36)
C(1)	0.3211 (10)	0.0	0.2500	0.0027 (7)	0.0835 (99)	0.0511 (73)	0.0	−0.0000	0.0313 (76)
C(2)	0.2839 (7)	0.0783 (17)	0.0706 (17)	0.0057 (006)	0.0385 (36)	0.0361 (38)	0.0000 (13)	−0.0042 (14)	0.0098 (34)

Location of the crystallographic axes and determination of the crystal system was not difficult since these polymorphs have coincident c axes, the needle axis of the crystal. The high-temperature form is orthorhombic with lattice constants of $a = 17.589$ (7) Å, $b = 7.296$ (3) Å, $c = 6.365$ (3) Å. For $Z = 4$, the calculated density is 1.89 g/cm^3, slightly *larger* than that of phase II. Intensity data were collected as above in the ranges $5° \leq 2\theta \leq 35°$ by using a scan width of 1.8° and a scan time of 2 s/step. The standard deviation of each reflection was calculated by using $\rho = 0.05$. Intensities of three standard reflections, checked every 45 reflections, remained constant. A total of 378 unique reflections with $F \geq 2.0\sigma(F)$ were used for structural refinement. The space group was determined as *Pcan* (an axial transform of *Pbcn*) by inspection of the diffractometer data which showed systematic absences of $h0l$, $h \neq 2n$, $0kl$, $l \neq 2n$, and $hk0$, $h + k \neq 2n$.

The structure was solved by using MULTAN,[19] a multisolution direct methods system. Copper and chlorine atomic positions were easily located from the calculated Fourier map of the most probable solution.

With $Z = 4$, the space group, *Pcan*, necessitates that the isopropylammonium ion be disordered, since there are eight general positions in this space group. The cations were found to be located on twofold rotation axes. As the IPA cation does not itself have a twofold symmetry, this placement is not physically reasonable without postulating disorder.

After refinement of the heavy atoms, nitrogen and carbon atoms were placed in positions located on the calculated difference map, and all atomic positional and anisotropic thermal parameters were refined. Hydrogen atom positions could not be located. R values, as defined above, were $R = 0.049$ and $wR = 0.055$. Maximum parameter shifts on the last cycle were one-fourth of their esd's. Final parameters are given in Table II. A table of observed and calculated structure factors is available.

Magnetic Susceptibility Measurements. The magnetic susceptibility of a 0.0924 g powdered sample of $IPACuCl_3$ was measured on a PAR vibrating sample magnetometer[20] between 4.2 and 60 K. The applied field was 5 kG and was calibrated by NMR techniques. The temperature was measured with a carbon-glass resistance thermometer, the calibration of which had been checked against the susceptibilities of several paramagnetic standards. The accuracy of the measurements is about 1%. Corrections to the data were made for diamagnetism and the temperature-independent paramagnetism of the copper ion.

A similar set of measurements were made on a quenched sample of phase I. A powdered sample (0.0951 g) was placed in a hot oil bath (80 °C) for 15 min, rapidly cooled to 78 K in a liquid-nitrogen bath, and then transferred to the liquid-helium cryostat of the magnetometer.

The susceptibility from 100 to 373 K was measured and reported as part of the M.S. thesis of M. Ahmed.[17] Upon comparing these data to the measurements described above, it became apparent that a scaling discrepancy existed between the two sets of data. To correct this, we loaded a 0.1510-g sample of $IPACuCl_3$ into a capsule and data were taken from 26 to 138 K. The data were corrected as above and agreed within error with the first data set collected on the VSM. The Ahmed data were scaled to agree with the VSM data in the overlapping region.

Electron Paramagnetic Resonance Experiments. Fixed-temperature spectra at room- and liquid-nitrogen temperatures were taken on a Varian E-3 spectrometer equipped with a Varian E-299 single-crystal orienter. Variable-temperature experiments were performed on the E-3 or on a Varian E-9 instrument equipped with a V-4540 EPR variable-temperature controller. Magnetic field magnitude and sweep width were calibrated before each use with DPPH, $H = 3388.4$ G at $\nu = 9.500$ gHz.

Powder samples were loaded into a capillary and placed along the axis of the microwave cavity. Single crystals used for EPR measurements were aligned and checked for singleness by using an X-ray precession camera and then mounted on a 2-mm glass rod.

Nuclear Magnetic Resonance Experiments. Broad-line NMR spectra were taken by using a Bruker SXP Pulse NMR spectrometer equipped with a BNC-12 computer. Because of the extremely short relaxation times and the necessity for fast data collection, intermediate data storage on a B-C 104 Transi-store was necessary. Temperature control was via a B-ST 100/700 Apparatus.

The sample was pulsed above the resonance at frequencies ranging from 90.31 to 90.11 MHz depending upon the relaxation rate and sample size. In general, a lower frequency was used for small samples and samples with slower relaxation times (narrower lines). The bandwidth was 1 MHz. The 90° pulse widths varied from 3.4 to 14 μs depending upon the pulse power available. Sweep widths were clculated as $^1/_2\Delta$ where Δ is the Transi-store dwell time.

Results

Phase II. As can be seen in Figures 1 and 2, the anion structure of phase II consists of nearly planar $Cu_2Cl_6^{2-}$ dimers linked by long axial Cu–Cl bonds to form bibridged linear chains of these dimers along the c crystallographic axis. The isopropylammonium cations are ordered and hydrogen bonded to one of the terminal chlorides, Cl(2). The other terminal chloride is connected by a long interaction to a copper in the adjacent dimer. Tables III and IV list bond distances and angles found in this structure.

The dimer is symmetrically bibridged, with Cu–Cl(1) distances of 2.301 (2) and 2.315 (2)Å. The third and fourth chloride ions in the copper coordination sphere are pulled downward slightly from a planar configuration by interactions with the cation and the neighboring dimers. The resulting values of θ, as defined

(19) G. Germain, P. Main, and M. M. Woolfson, *Acta Crystallogr., Sect. A*, **A27**, 368 (1971).
(20) C. P. Landee, S. A. Roberts, and R. D. Willett, *J. Chem. Phys.*, **68**, 4574 (1978).

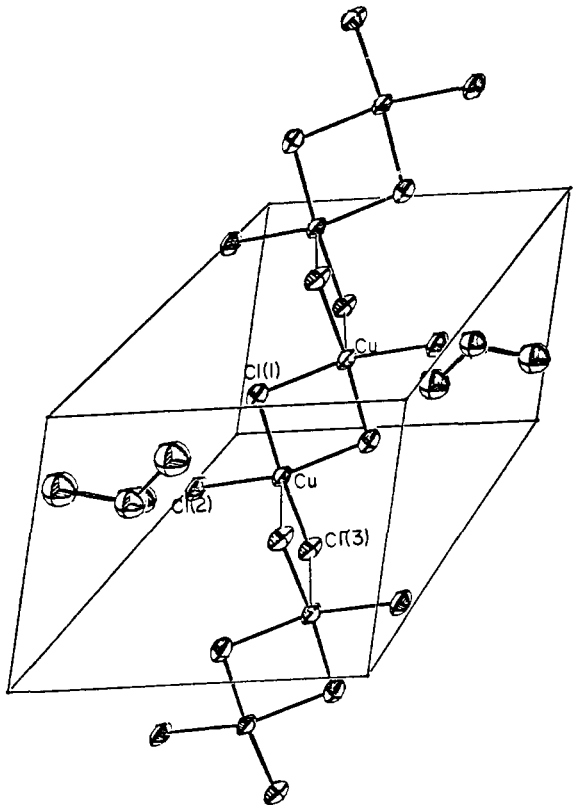

Figure 1. Unit-cell contents and ajacent dimers of phase II of $IPACuCl_3$. The *b* axis is horizontal and the *a* axis vertical.

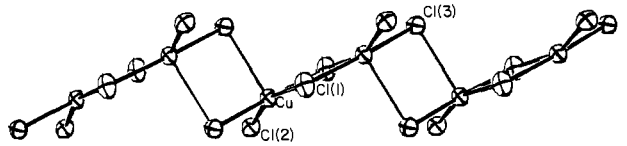

Figure 2. A side view of phase II $IPACuCl_3$ dimer showing the planarity of the $Cu_2Cl_6^{2-}$ dimers. The *c* axis is horizontal. The view is roughly from the *b* direction.

Table III. Bond Distances (Å) and Angles (Deg) in $Cu_2Cl_6^{2-}$ Dimer System of $IPACuCl_3$ Phase II

	Bond Distances		
Cu-Cl(1)	2.301 (2)	Cu-Cl(3)	2.699 (2)
Cu-Cl(1)	2.315 (1)	Cu-Cu[a]	3.417 (1)
Cu-Cl(2)	2.273 (2)	Cu-Cu[b]	3.506 (2)
Cu-Cl(3)	2.269 (1)		
	Bond Angles		
Cl(1)-Cu-Cl(3)[c]	100.56 (6)	Cl(2)-Cu-Cl(1)	160.53 (8)
Cl(1)-Cu-Cl(3)[c]	91.87 (6)	Cl(3)-Cu-Cl(3)[c]	90.65 (5)
Cl(1)-Cu-Cl(1)	84.79 (6)	Cl(3)-Cu-Cl(1)	175.10 (9)
Cl(2)-Cu-Cl(3)[c]	98.42 (7)	Cl(3)-Cu-Cl(1)	90.91 (6)
Cl(2)-Cu-Cl(1)	90.60 (6)	Cl(3)-Cu-Cl(2)	93.19 (5)
Cu-Cl(1)-Cu	95.51 (6)	Cu-Cl(3)-Cu	89.35 (5)

[a] Intradimer bond length. [b] Interdimer length. [c] Apical Cl(3).

earlier, are 160.53 (8) and 175.10 (9)°. Cl(2), at a distance of 2.273 (2)Å from the copper, is very strongly hydrogen bonded to the IPA cation, with the hydrogen-bonding distances (Cl-H) being 2.45 (10) and 2.55 (12) Å. The deviation of the dimer from planarity is 19.5°. Cl(3) is hydrogen bonded to the cation but also has a long interaction of 2.699 (2)Å with the nearest copper in the adjacent dimer. Thus, each copper is surrounded by five chlorides in a nearly square-pyramidal arrangement. The two symmetric bridging chlorines and the two "terminal" chlorines are in the plane of the copper atoms, and an apical long-bonded interaction exists to a chloride belonging to the next dimer. The structure of the dimer is nearly identical with that found in $(CH_3)_2NH_2CuCl_3$[21a] but more distorted from planarity than those

Table IV. Bond Distances (Å) and Angles (Deg) in IPA Cation Phase II

atoms	distance	atoms	angle
N-H(2)	0.82 (10)	C(1)-N-H(1)	112 (8)
N-H(1)	0.84 (11)	C(1)-N-H(2)	109 (8)
N-H(3)	1.05 (13)	C(1)-N-H(3)	112 (5)
N-C(1)	1.503 (8)	H(1)-N-H(2)	111 (9)
		H(1)-N-H(3)	89 (11)
		H(2)-N-H(3)	121 (8)
N-C(1)	1.503 (8)	N-C(1)-C(2)	107.8 (5)
C(1)-C(2)	1.53 (1)	N-C(1)-C(3)	109.8 (7)
C(1)-C(3)	1.49 (1)	N-C(1)-H(4)	104 (4)
C(1)-H(4)	1.06 (11)	C(2)-C(1)-C(3)	113.8 (5)
		C(2)-C(1)-H(4)	108 (6)
		C(3)-C(1)-H(4)	112 (5)
C(2)-C(1)	1.53 (1)	C(1)-C(2)-H(5)	120 (4)
C(2)-H(5)	1.06 (11)	C(1)-C(2)-H(6)	105 (8)
C(2)-H(6)	0.84 (12)	C(1)-C(2)-H(7)	113 (5)
C(2)-H(7)	1.03 (10)	H(5)-C(2)-H(6)	118 (8)
		H(5)-C(2)-H(7)	94 (8)
		H(6)-C(2)-H(7)	105 (8)
C(3)-C(1)	1.49 (1)	C(1)-C(3)-H(8)	120 (5)
C(3)-H(8)	1.05 (12)	C(1)-C(3)-H(9)	117 (6)
C(3)-H(9)	0.88 (11)	C(1)-C(3)-H(10)	118 (7)
C(3)-H(10)	1.06 (8)	H(8)-C(3)-H(9)	92 (10)
		H(8)-C(3)-H(10)	102 (7)
		H(9)-C(3)-H(10)	101 (7)

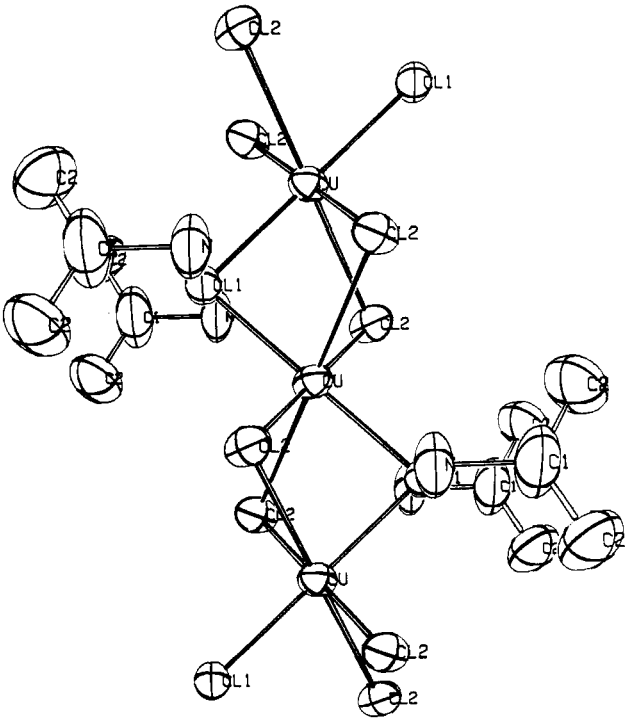

Figure 3. The structure of phase I of $IPACuCl_3$ viewed from the *b* direction.

found in $KCuCl_3$ and NH_4CuCl_3.[21b] Bulkier cations without hydrogen-bonding capability yield isolated dimers with pronounced tetrahedral distortion of the copper coordination geometry.[22]

From Table III, it can be seen that the difference in the intradimer copper–copper distance of 3.417 (1) Å and the interdimer distance of 3.506 (2) Å is small. Another way of looking at this structure is as a zig-zag arrangement of copper ions connected alternately by two symmetric chloride bridges (what has been referred to here as a dimer) and by two asymmetric chloride

(21) (a) R. D. Willett, *J. Chem. Phys.*, **44**, 39 (1966). (b) R. D. Willett, C. Dwiggens, Jr., R. F. Kruh, and R. E. Rundle, *J. Chem. Phys.*, **38**, 2429 (1963).

(22) R. D. Willett and C. Chow, *Acta Crystallogr. Sect. B*, **B30**, 207 (1974).

Table V. Bond Distances (Å) and Angles (Deg) in $IPACuCl_3$, Phase I

	Bond Distances		
Cu–Cl(1)	2.337 (2)	Cu–Cu	3.182
Cu–Cl(2)	2.290 (2)	N–C(1)	1.47 (2)
Cu–Cl(2)	2.860 (2)	C(1)–C(2)	1.44 (1)
	Bond Angles		
Cl(2)–Cu–Cl(1)	90.91 (7)	Cu–Cl(1)–Cu	85.8 (1)
Cl(2)–Cu–Cl(2)	86.90 (9)	Cu–Cl(2)–Cu	75.44 (7)
Cl(1)–Cu–Cl(2)	103.44 (6)	C(2)–C(1)–C(2)	126 (2)
		C(2)–C(1)–N	117 (1)

Table VI. Root-Mean-Square Amplitudes (Å) of Thermal Motion along the Principle Axes of Vibration in Both Phases of $IPACuCl_3$

	$U_1^{1/2}$	$U_2^{1/2}$	$U_3^{1/2}$
	Phase II		
Cu	0.130	0.184	0.206
Cl(1)	0.143	0.191	0.264
Cl(2)	0.147	0.193	0.230
Cl(3)	0.152	0.193	0.222
N	0.177	0.199	0.244
C(1)	0.170	0.200	0.244
C(2)	0.207	0.244	0.266
C(3)	0.199	0.253	0.272
	Phase I		
Cu	0.173	0.187	0.222
Cl(1)	0.187	0.195	0.230
Cl(2)	0.178	0.202	0.265
N	0.180	0.238	0.342
C(1)	0.206	0.264	0.510
C(2)	0.223	0.310	0.349

bridges (the interdimer interaction). Since the crystal system is triclinic with one dimer per cell, each dimer in the crystal lies parallel to every other dimer and all of these dimer chains run parallel to each other. This is in contrast to the structure of the nonthermochromic dimethylammonium trichlorocuprate(II) salt[21a] in which the chains of copper atoms are puckered and the parallel dimer alignment does not exist.

Phase I. As shown in Figure 3, phase I contains linear chains of copper ions located upon crystallographic inversion centers. Each pair of copper ions is bridged by one symmetric and two asymmetric Cl bridges. The distances are shown in Table V. Each copper is octahedrally coordinated to six chlorides, with the identical bonds being in trans positions. Thus, the coordination number is *larger* in phase I than in phase II, a result not anticipated from thermodynamic considerations. These $(CuCl_3)_n^{n-}$ chains run parallel to the crystallographic *c* axis, which is coincident with the *c* axis of phase II. As can be seen from Table VI, there is no more thermal motion in the anionic system of phase I than in the dimer of phase II and there is no abnormally high amplitudes of vibration for Cu or Cl in either phase. The overall structure of the anion in phase I is quite similar to that of the $CuCl_3$ chain found in trimethylammonium heptachlorodicuprate(II).[23]

The location of the cation atoms in this structure must be addressed more precisely. The space group requires that the IPA cations must be disordered and the disorder must have twofold rotational symmetry. It might be expected to find locations on the electron density map for two superimposed IPA cations, which when combined, would produce the required rotational symmetry. However, no discrete atomic positions for two disordered cations could be found. The best locations on the Fourier map for the cation atoms are in those chemically impossible positions. The relatively short bond distances found in the cation are characteristic of distances in an averaged structure, and the thermal parameters of the cation carbon atoms are correspondingly large. Disordered cation positions could have been postulated from this model, but because only a small number of reflections were collected due to rapid fall off of intensity with Bragg angle, the refinement of these positions would be meaningless. As shown by the close N–Cl(2) contacts listed in Table VII, the cation in phase I is still hydrogen bonded to the anion system. However, a significant lengthening of the N–Cl distances does occur, indicating a weakening of the hydrogen bonding.

(23) R. M. Clay, P. Murray-Rust, and J. Murray-Rust, *J. Chem. Soc., Datlon Trans.*, 595, 1973 (1973).

Table VII. Closest Hydrogen-Bonding Contacts (Å) in $IPACuCl_3$

atoms	distance	atoms	distance
Cl(2)–NH(2)	2.55 (12)	Cl(3)–NH(1)	2.53 (10)
Cl(2)–NH(3)	2.46 (10)		
Cl(2)–N[a]	3.261 (6)	Cl(2)–N	3.397 (7)
Cl(2)–N	3.319 (7)	Cl(3)–N	3.333 (6)
	Phase I		
Cl(2)–N	3.33 (1)	Cl(2)–N	3.40 (1)

[a] Nonhydrogen-bonding interaction.

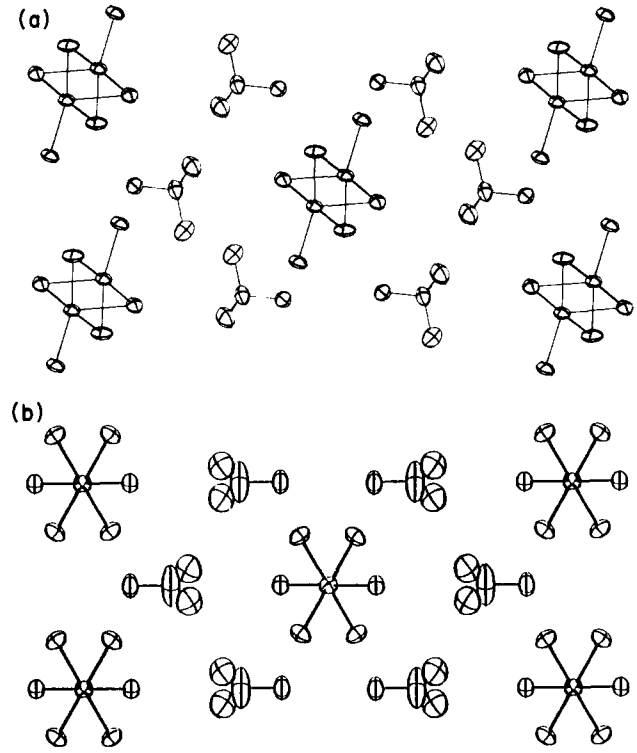

Figure 4. A projection of the structures of both phases of $IPACuCl_3$ down the coincident *c* axis. (a) is the phase II while (b) is phase I.

Relationship between the Structures. The significant feature in comparing the two phases appears to be the competition between the ammonium group and the copper(II) ion for bonding with Cl(2). In phase II, the strong hydrogen bonding to Cl(2) preculdes the formation of a second Cu–Cl(2) bond. Thus, the copper(II) ion is five-coordinate, and the resultant, rather open, bibridged linear chain is formed. In phase I, the hydrogen bonding is weaker, the copper(II) ion is able to use Cl(2) to complete its distorted octahedrons, and this leads to the more compact tribridged chain. It is noted that the volume change, ΔV, is nearly zero for the transition. Thus the increased volume due to the dynamic nature of the disorder (vide infra) is just equal to the shrinkage in volume of the copper chloride chain.

This transformation can be visualized with the aid of Figure 4, which shows projections of both structures down the *c* axis. If the hydrogen-bonding constraint is reduced at Cl(2) and the copper atoms allowed to move toward a linear configuration, Cl(2) will approach the next copper, distorting its ligand arrangement into a six-coordinate array. This will force the Cl(2) from that copper to fold backward and approach the next copper down the chain. Although the copper coordination change appears at first glance to be drastic, the difference between the anion configurations is structurally quite small, only requiring the release of the hydrogen-bonded chloride ion and the movement of each copper by

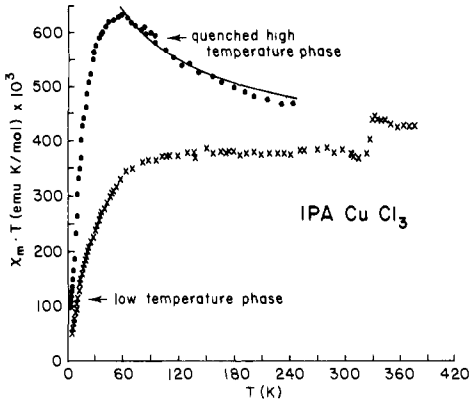

Figure 5. Magnetic susceptibility of $IPACuCl_3$ plotted as $\chi_m T$ from 4 to 373 K. The data above 140 K are rescaled from ref 17.

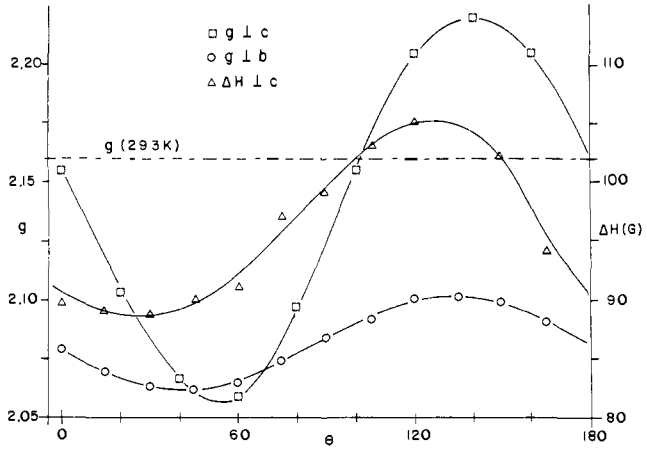

Figure 6. EPR **g** tensor and line width behavior of $IPACuCl_3$ at 77 K.

about 0.25 Å, an amount accounted for by thermal motion at room temperature.

Magnetic Susceptibility Results. From the structural results and superexchange arguments, phase II is expected to be antiferromagnetically coupled since the bridging angle of the symmetically bridged chlorides is 95.51 (6)°.[24] The interaction through the other chlorides is more difficult to predict due to the asymmetry in the bridging bond lengths, but a net antiferromagnetic interaction is expected. Phase I is a tribridged linear chain with Cu–Cl–Cu bridging angles of 85.8 (1)° (symmetric) and 75.44 (7)° (asymmetric), so that a ferromagnetic interaction is expected. This is of great interest since one-dimensional spin $^1/_2$ Heisenberg ferromagnets have, until very recently, been elusive.[25]

Figure 5 illustrates a plot of χT vs. T for the two phases of $IPACuCl_3$. The data for phase II shows the existence of a net antiferromagnetic coupling at low temperatures. The quenched phase data show typical behavior for a quasi-one dimensional system with strong ferromagnetic intrachain coupling and substantial antiferromagnetic interchain coupling. The moment (proportional to the square root of χT) first increases as T is decreased, due to the intrachain interactions, and then decreases as the weaker interchain interactions start coupling the chains together antiferromagnetically.

The phase II data below 60 K have been analyzed by using several models including 1-D Ising, 1-D Heisenberg, isolated dimer, and mean field dimer models, all giving extremely poor fits to the

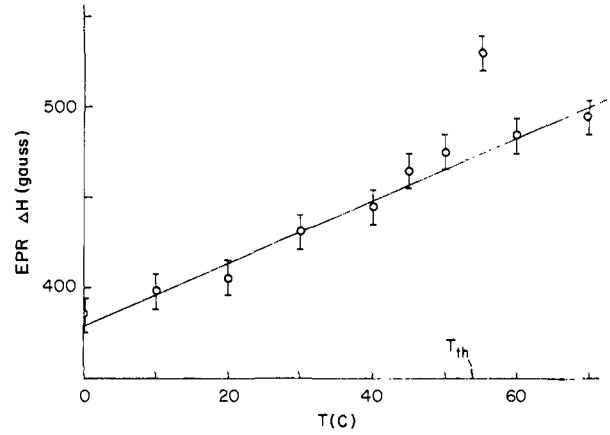

Figure 7. Temperature dependence of the EPR line width of $IPACuCl_3$ near T_{th}. The line width shows divergence near T_{th}, but the instrument temperature control is not good enough to quantify it.

experimental results; the last two indicating that the structure is indeed not a simple dimer as a first glance at the X-ray results would seem to indicate.The best fit to this data was obtained as a fit to an alternate Ising model, with the susceptibility given by eq 1.[26] In this expression, J_1 is the intradimer exchange interaction

$$\chi = \frac{C}{T}\exp\left(\frac{J_1}{2KT} + \frac{J_2}{2KT}\right) \Big/ \cosh\left(\frac{J_1}{2KT} + \frac{J_2}{2KT}\right) \qquad (1)$$

and J_2 the interdimer exchange, which is not equal to J_1. The fit to the model yields $J_1 = -23$ K and $J_2 = -9$ K, with a residual of only 1.5%. Unfortunately, due to the symmetry of the expression, attempts to refine these values using the least-squares procedure were not successful. The values for J were arrived at by trial and error. Only poor fits were obtained with a positive J_2, indicating that an antiferromagnetic interdimer interaction is present.

The quenched phase data was fit to a model for a one-dimensional Heisenberg ferromagnet,[27] corrected for interchain interactions with a mean field model.[25] This yielded a ferromagnetic intrachain coupling constant of $J/k = 58$ (6) K and an antiferromagnetic constant of $ZJ/k = -9$ (1) K, where Z = number of neighboring chains. The interchain coupling undoubtably arises through hydrogen-bonding pathways, so $Z = 2$. Again, the quality of the agreement between model and experiment is not outstanding, but this is largely attributable to the failure of the mean field corrections for such a large $|J'/J|$ ratio.

The susceptibility at T_{th} shows a sudden, sharp break with no evidence of premonitory behavior, indicating an isothermal, first-order phase transition.[17] The increase in χ of 15% at T_{th} is consistent with the transformation from an antiferromagnetic to a ferromagnetic system.

Magnetic Resonance Experiments. So far, the evidence presented has established the structure of the phases and the relationship between them and has enabled a determination to be made of the structural change occurring at T_{th}. To this point, no experiments have been described which would determine the processes involved in the phase transition. By studying the EPR and the ^1H NMR spectra of $IPACuCl_3$, the thermal motions of metal–halogen framework and the organic cation, respectively, can perhaps be unravelled and a conjecture made about the mechanism of the phase transition.

EPR Experiments. Single-crystal EPR spectra taken on X-ray oriented crystals at liquid-nitrogen temperature show the behavior predicted from the crystal structure results, that is both g and the line width show anisotropic behavior. Figure 7 summarizes these results. It should be pointed out that because the crystal is triclinic, the principal axes of the **g** tensor are not required to lie along the

(24) W. E. Hatfield, in "Extended Interactions between Metal Ions", Leonard V. Interrante, Ed., American Chemical Society, Washington, DC, 1974, p 108.

(25) D. D. Swank, C. P. Landee, and R. D. Willett, *Phys. Rev. B*, **20**, 2154 (1978); C. P. Landee and R. D. Willett, *Phys. Rev. Lett.*, **43**, 463 (1979); R. D. Willett, C. P. Landee, R. M. Gaura, D. D. Swank, H. A. Groenedijk, and A. J. van Duyneveldt, *J. Magn. Magn. Mater.*, **15–18**, 1055 (1980).

(26) M. Inoue and M. Kubo, *J. Magn. Reson.*, **4**, 1975 (1971).

(27) J. Bonner and M. E. Fisher, *Phys. Rev.*, **135**, A640 (1964).

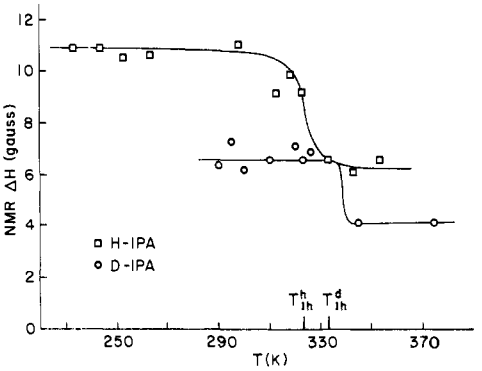

Figure 8. Temperature dependence of the NMR line width for H-IPA-$CuCl_3$ and D-IPA$CuCl_3$. Within the error of the measurements, the narrowing occurs discontinuously at T_{th}.

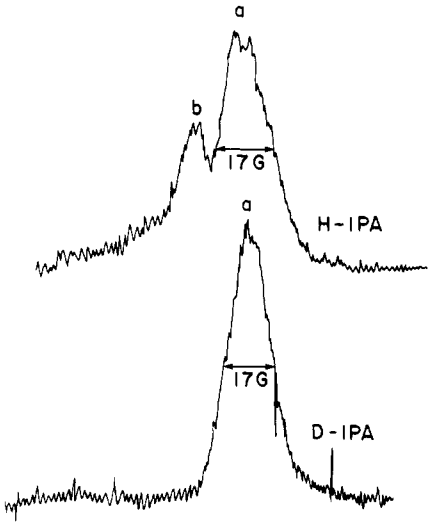

Figure 9. ^1H NMR of H-IPA$CuCl_3$ and D-IPA$CuCl_3$ at 123 K. The a resonances are C–H protons while the b resonances are due to the N–H protons in the undeuterated salts.

crystallographic axes. No attempt was made to quantitatively characterize the **g** tensor since only the anisotropy at 77 K is important in light of the following results. However, since the psuedo C_4 axis of each copper(II) ion lies closest to the *a* axis, we expect $g_{max} = g_{\parallel}$ to be approximately parallel to *a*, with $g_{min} \approx g_{\perp}$ along *b* and *c*. This is as observed.

The EPR spectra of a powdered sample of IPA$CuCl_3$ were measured as the sample temperature was raised through T_{th}. No change occurs in *g*, but, as shown in Figure 8, the line width broadens at T_{th}. This broadening is anticipated due to the reorientation processes taking place during the transition. The temperature dependence of line width is the same in both phases. Thus, the processes leading to the temperature dependence, which are beyond the scope of this study, are likely to be the same in both phases.

NMR Experiments. Broad-line studies were performed on IPA$CuCl_3$ and D-IPA$CuCl_3$ as pictured in Figure 9, both salts show a discontinuous narrowing of the line at T_{th} with only one line being observed above 230 K for either sample. The phase transition and the narrowing of the NMR line occur at the same temperature within the accuracy of the data. Unfortunately, the best temperature control obtained consistently was only ±3 °C so data close to T_{th} could not be obtained. However, when the FID is watched on the oscilloscope, the change at the phase transition occurs within 1 pulse time (1 s). Thus, it is apparent that the line width changes discontinuously. All T_2 values were calculated from fitting the FID to either an exponential or Gaussian decay function, and the line width values calculated from T_2 compare well with those obtained from the spectra. The magnitude of the ΔH narrowing at T_{th} is consistent with that previously seen for a twofold rotation of the cation system about the N–C axis.[28] Certainly the narrowing is much less than that expected for "free" rotation of the cation, which would give a line width on the order of 2–3 G, not the 4.5 G observed for D-IPA-$CuCl_3$. Thus, the NMR results show that the cation disorder seen in the X-ray study is of a dynamic nature.

It is observed that the transition occurs about 10 °C higher for the deuterated salt than for the nondeuterated compound. Since the transition is a first-order discontinuous phase transition and not a activated process, this can be rationalized by the following argument. The hydrogen bond strength is given by $D_0 - {}^1/_2h\nu$, the dissociation energy of the N–H···Cl bond less the vibrational energy in the system. At the point where the energetic considerations are such that $G_{\mathrm{I}} = G_{\mathrm{II}}$, the phase transition occurs. Given stronger hydrogen bonding in phase II, we have $\nu_{\mathrm{I}}{}^{\mathrm{H}} < \nu_{\mathrm{II}}{}^{\mathrm{H}}$. With the assumption of equal hydrogen bond energies (D_0) for IPA-$CuCl_3$ and D-IPA$CuCl_3$ and the same structures, the deuterated salt of the two phases will be stabilized by the amount $\nu_{\mathrm{I}}{}^{\mathrm{H}} - \nu_{\mathrm{I}}{}^{\mathrm{D}}$ and $\nu_{\mathrm{II}}{}^{\mathrm{H}} - \nu_{\mathrm{II}}{}^{\mathrm{D}}$, respectively. The ratio $\nu_i{}^{\mathrm{H}}/\nu_i{}^{\mathrm{D}}$ is given by eq 2,

$$\nu_i{}^{\mathrm{H}}/\nu_i{}^{\mathrm{D}} = \sqrt{\mu_i{}^{\mathrm{D}}}\Big/\sqrt{\mu_i{}^{\mathrm{H}}} \qquad (2)$$

where $\mu_i{}^{\mathrm{H}}$ and $\mu_i{}^{\mathrm{D}}$ are the reduced mass of the vibrational system for the hydrogen bonds. With the assumption that the ratio $\mu_i{}^{\mathrm{D}}/\mu_i{}^{\mathrm{H}}$ is the same in the two phases, it is concluded that $\nu_{\mathrm{I}}{}^{\mathrm{H}} - \nu_{\mathrm{I}}{}^{\mathrm{D}} < \nu_{\mathrm{II}}{}^{\mathrm{H}} - \nu_{\mathrm{II}}{}^{\mathrm{D}}$, so that phase II is stabilized more than phase I by deuteration. Thus, the deuteration data corroborate the interpretation of the X-ray data that the weaker hydrogen bond in phase I is the crucial factor in describing the phase transition.

Finally, it should be noted that as the temperature is lowered, the NMR line width at first increases proportional to $1/T$, and then at low temperatures in the H-IPA (but not D-IPA) salt, a line splits out from the main resonance to higher fields. The temperature dependence of the line width below T_{th} is due to an increase in the dipolar broadening from the electron magnetic moment (μ_e). In this region, the temperature dependence of μ_e is described by the Curie Law and increases proportional to $1/T$. As shown in Figure 9, comparison of the H-IPA and D-IPA spectra at 123 K (the lowest temperature obtainable) shows that the high-field peak is due to the N–H resonances, which are split out due to a larger Fermi-contact shift of those protons by the paramagnetic electrons.[29]

Conclusion

The solid-state phase transition in IPA$CuCl_3$ occurs at 51 °C for the H-IPA salt and 61 °C for the D-IPA salt. X-ray crystal structure results show that the structural change between the two crystal forms is from a bibridged chain of dimers to a tribridged chain with a disordered cation in the higher temperature phase. Visual observation of the transition and the susceptibility results indicate the discontinuity of the transition and allow the classification of this phase transition as first order. The proton NMR data confirm the first-order nature of the transition and that a dynamic twofold disorder of the IPA ion exists in phase I. No evidence for unusual disorder or thermal motion of the anionic chains is found for either phase I or phase II.

Thermodynamically, phase I is stabilized at high temperatures because of its larger entropy associated with the dynamic disorder of the IPA^+ cation. Conversely, phase II is more stable at low temperature due to its greater lattice energy. This is primarily due to the difference in hydrogen bond strengths in the two phases. Upon onset of hindered rotation, the IPA^+ ion occupies a larger volume in the lattice, weakening the N–H···Cl interactions, particularly to Cl(2). This allows each copper(II) ion to increase its coordination number to six by including a second Cl(2) ion in its coordination sphere. Thus, the high-temperature phase contains the more compact copper chloride framework, a most surprising and unusual result.

(28) R. Sjoblom and J. Tegenfeldt, *Acta Chem. Scand.*, **26**, 3068 (1972).
(29) A. Abragam, "The Principals of Nuclear Magnetism", Oxford University Press, London, 1961, pp 159 ff.

Acknowledgment. This research was supported by NSF. The access to susceptibility data from the M.S. thesis of M. Ahmed and discussions with his thesis supervisor, Professor M. Mostafa, is gratefully acknowledged.

Supplementary Material Available: Listings of observed and calculated structure factor amplitudes for $(CH_3)_2CHNH_3CuCl_3$ in phases I and II (4 pages). Ordering information is given on any current masthead page.

Thermochromism in Copper(II) Halide Salts. 2. Bis(isopropylammonium) Tetrachlorocuprate(II)

Darrel R. Bloomquist,* Roger D. Willett, and Harold W. Dodgen

Contribution from the Department of Chemistry, Washington State University, Pullman, Washington 99164. *Received July 21, 1980*

Abstract: Bis(isopropylammonium) tetrachlorocuprate(II) is thermochromic, undergoing a first-order phase transition at T_{th} = 50 °C, changing from green to yellow. The structure of the high-temperature phase (orthorhombic, *Pnma*, a = 16.007 (4) Å, b = 12.262 (3) Å, and c = 7.784 (2) Å, Z = 4) has been determined and shown to contain distorted tetrahedral $CuCl_4^{2-}$ anions and disordered isopropylammonium cations. Cu–Cl distances range from 2.204 to 2.218 Å, with trans Cl–Cu–Cl angles = 134.3° and 135.3°. The previously determined room-temperature structure consists of ribbons of five- and six-coordinate copper ions based on the laminar $(RNH_3)_2CuCl_4$ structures. DSC studies yield ΔH_{th} = 2.9 kcal/mol and ΔS_{th} = 9.0 cal/(mol deg) for the transition. The value of ΔS_{th} is consistent with the disorder of the cations and the drastic rearrangement of the cationic structure. Broad-line ^1H NMR measurements show that the anion disorder is dynamic in nature. The second moment of the NMR line drops discontinuously from 7.8 to 4.8 G^2 at the phase transition. This is in quantitative agreement with theoretical second moments based on the disorder observed in the high-temperature phase. The EPR spectrum also shows a discontinuous change at the phase transition. Magnetic susceptibility studies on the quenched high-temperature phase show the existence of extremely weak antiferromagnetic coupling between the $CuCl_4^{2-}$ ions, probably occurring via hydrogen bonding. The data all strongly support the hypothesis that the thermochromism in copper halides is driven entropically by the onset of dynamic disorder of the organic cations. The weakening of the hydrogen bonding destabilizes the low-temperature stereochemistry, allowing, in most cases, the copper halide salt to distort toward tetrahedral geometry.

In a series of papers, we have investigated the phenomenon of thermochromism in copper halide salts. In particular, emphasis has been on those salts in which the color change is associated with a change in stereochemistry brought about by the presence of a structural phase transition. Spectroscopically, it has shown that the color change is associated with a relaxation of the stereochemistry from a square-planar (or square-pyramidal or square-bipyramidal) geometry toward a tetrahedral geometry.[1-3] Structurally, this has been verified for $(PhCH_2NH_2CH_3)_2CuCl_4$.[4] A counter example to this was shown to exist in $[(CH_3)_2CHNH_3]CuCl_3$, where the coordination geometry *increased* from square pyramidal to square bipyramidal.[5] A subsequent study of the corresponding bromide salt showed the existence of an additional phase in which a distortion toward tetrahedral geometry apparently exists.[6] In the latter studies, it was shown that the phase transitions were driven entropically by the onset of dynamic disorder of the organic cations. Hydrogen bonding is thus weakened in the high-temperature phase, allowing electrostatic effects to dominate over crystal field stabilization in the determination of the stereochemistry.

In this paper, the structure and magnetic behavior of the high-temperature phase of $[(CH_3)_2CHNH_3]_2CuCl_4$, henceforth $(IPA)_2CuCl_4$, is reported, along with a DSC, ^1H NMR, and EPR study of the phase transition.

Experimental Section

Crystals of the room-temperature phase (phase II) of $(IPA)_2CuCl_4$ grow as fine straw green needles from methanol, ethanol, or aqueous solutions containing stoichiometric amounts of the hydrochloride salt of isopropylamine and cupric chloride dihydrate as described by Remy and Laves.[7] Much larger single crystals of higher purity can be obtained upon slow evaporation from *n*-propyl alcohol. This compound can also be prepared as a fine powder by adding ether to a saturated ethanolic solution. The high-temperature phase (phase I) grows as yellow, rectangular platelets from hot alcoholic solutions.

DTA and DSC measurements were carried out on a Du Pont 900 thermal analyzer. The ^1H continuous-wave NMR measurements were made with an instrument with a phase-sensitive detection design incorporating a PAR lock-in amplifier and a Varian V4210A variable-frequency R-F unit. Data were recorded, while sweeping the magnetic field, with a FabriTech 1052 LSH 1024 point signal averager interfaced with a Motorola microprocessor previously described. The EPR spectra were recorded on a Varian E-3 spectrometer. A liquid-circulation temperature-control system designed to fit either instrument was used for precise temperature regulation from 20 to 100 °C.[8] Dow Corning 200 electronic fluid functions satisfactorily as the thermal liquid for EPR measurements while perfluorotributylamine was found to be the ideal liquid for ^1H NMR experiments. Magnetic susceptibility studies were carried out on a PAR vibrating sample magnetometer. The same techniques previously described were utilized for obtaining data on the quenched high-temperature phase.[5] A 0.1086-g sample was used and diamagnetic corrections (-126×10^{-6} emu/mol) and TIP paramagnetic corrections (60×10^{-6} emu/mol) were applied.

The crystalline properties of a single crystal of $(IPA)_2CuCl_4$ are destroyed during the phase transition. Freshly prepared room-temperature

* To whom correspondence should be addressed at Hewlett-Packard, Disc Memory Division, Boise, Idaho 83707.

(1) R. D. Willett, J. A. Haugen, J. Lebsack, and J. Morrey, *Inorg. Chem.*, **13**, 2510 (1974).
(2) G. Marcotrigiano, L. Menabue, and G. C. Pellacani, *Inorg. Chem.*, **15**, 2333 (1976).
(3) R. D. Willett, J. R. Ferraro, and M. Choca, *Inorg. Chem.*, **13**, 2919 (1974).
(4) R. L. Harlow, W. J. Wells, III, G. W. Watt, and S. H. Simonsen, *Inorg. Chem.*, **13**, 2106 (1974).
(5) S. A. Roberts, D. R. Bloomquist, R. D. Willett, and H. W. Dodgen, *J. Am. Chem. Soc.*, to be submitted for publication.
(6) D. R. Bloomquist, R. D. Willett, and H. W. Dodgen, *J. Am. Chem. Soc.*, to be submitted for publication.
(7) H. Remy and G. Laves, *Ber.*, **66**, 401 (1933).
(8) D. R. Bloomquist and H. W. Dodgen, to be submitted for publication.

0002-7863/81/1503-2610$01.25/0